AMERICAN SOCIETY FOR MICROBIOLOGY | Applied and Environmental Microbiology®

BIOTECHNOLOGY

Production of 2-Hydroxyisobutyric Acid from Methanol by *Methylobacterium extorquens* AM1 Expressing (*R*)-3-Hydroxybutyryl Coenzyme A-Isomerizing Enzymes

Maria-Teresa Rohde, Sylvi Tischer, Hauke Harms, Thore Rohwerder

Helmholtz Centre for Environmental Research-UFZ, Department of Environmental Microbiology, Leipzig, Germany

ABSTRACT The biotechnological production of the methyl methacrylate precursor 2-hydroxyisobutyric acid (2-HIBA) via bacterial poly-3-hydroxybutyrate (PHB) overflow metabolism requires suitable (*R*)-3-hydroxybutyryl coenzyme A (CoA)-specific coenzyme B_{12}-dependent mutases (RCM). Here, we characterized a predicted mutase from *Bacillus massiliosenegalensis* JC6 as a mesophilic RCM closely related to the thermophilic enzyme previously identified in *Kyrpidia tusciae* DSM 2912 (M.-T. Weichler et al., Appl Environ Microbiol 81:4564–4572, 2015, https://doi.org/10.1128/AEM.00716-15). Using both RCM variants, 2-HIBA production from methanol was studied in fed-batch bioreactor experiments with recombinant *Methylobacterium extorquens* AM1. After complete nitrogen consumption, the concomitant formation of PHB and 2-HIBA was achieved, indicating that both sets of RCM genes were successfully expressed. However, although identical vector systems and incubation conditions were chosen, the metabolic activity of the variant bearing the RCM genes from strain DSM 2912 was severely inhibited, likely due to the negative effects caused by heterologous expression. In contrast, the biomass yield of the variant expressing the JC6 genes was close to the wild-type performance, and 2-HIBA titers of 2.1 g $liter^{-1}$ could be demonstrated. In this case, up to 24% of the substrate channeled into overflow metabolism was converted to the mutase product, and maximal combined 2-HIBA plus PHB yields from methanol of 0.11 g g^{-1} were achieved. Reverse transcription-quantitative PCR analysis revealed that metabolic genes, such as methanol dehydrogenase and acetoacetyl-CoA reductase genes, are strongly downregulated after exponential growth, which currently prevents a prolonged overflow phase, thus preventing higher product yields with strain AM1.

IMPORTANCE In this study, we genetically modified a methylotrophic bacterium in order to channel intermediates of its overflow metabolism to the C_4 carboxylic acid 2-hydroxyisobutyric acid, a precursor of acrylic glass. This has implications for biotechnology, as it shows that reduced C_1 substrates, such as methanol and formic acid, can be alternative feedstocks for producing today's commodities. We found that product titers and yields depend more on host physiology than on the activity of the introduced heterologous function modifying the overflow metabolism. In addition, we show that the fitness of recombinant strains substantially varies when they express orthologous genes from different origins. Further studies are needed to extend the overflow production phase in methylotrophic microorganisms for the implementation of biotechnological processes.

KEYWORDS acyl-CoA mutase, bulk chemicals, fed-batch bioreactor, overflow metabolism, polyhydroxybutyrate

Received 15 September 2016 **Accepted** 8 November 2016

Accepted manuscript posted online 11 November 2016

Citation Rohde M-T, Tischer S, Harms H, Rohwerder T. 2017. Production of 2-hydroxyisobutyric acid from methanol by *Methylobacterium extorquens* AM1 expressing (*R*)-3-hydroxybutyryl coenzyme A-isomerizing enzymes. Appl Environ Microbiol 83:e02622-16. https://doi.org/10.1128/AEM.02622-16.

Editor Hideaki Nojiri, The University of Tokyo

Address correspondence to Thore Rohwerder, thore.rohwerder@ufz.de.

To entirely replace petrochemical processes relying on fossil resources in the near future, the development of a biology-based economy involving the production of industrial bulk chemicals by genetically engineered microorganisms becomes increasingly important. In this connection, key platform chemicals producible in commercialized microbial fermentation processes have been announced, including succinic acid, lactic acid, 3-hydroxypropionic acid, and ethanol (1, 2). However, due to the discovery of 2-hydroxyisobutyryl coenzyme A (CoA) mutase (HCM) (3, 4), 2-hydroxyisobutyric acid (2-HIBA), a hydroxylated carboxylic acid containing a tertiary carbon atom, is a further building block with a high potential for use in industry. HCM was originally found in *Aquincola tertiaricarbonis* L108, a bacterial strain capable of degrading the fuel oxygenate methyl *tert*-butyl ether (5). It was classified as a coenzyme B_{12}-dependent acyl-CoA mutase and shown to specifically isomerize 3-hydroxybutyryl-CoA into 2-hydroxyisobutyryl-CoA (3). On the basis of this reaction, the polyhydroxybutyrate (PHB) pathway, a prevalent overflow metabolic pathway of bacteria (6), could be employed for biotechnological 2-HIBA production (7). In this pathway (Fig. 1), the common metabolite acetyl-CoA is converted into (*R*)-3-hydroxybutyryl-CoA by beta-ketothiolase (PhaA) and NADPH-dependent acetoacetyl-CoA reductase (PhaB). Then, instead of the ensuing polymerization step catalyzed by PHB polymerase (PhaC), HCM can generate 2-hydroxyisobutyryl-CoA, which is subsequently cleaved by intracellular thioesterases and excreted as 2-HIBA. The latter can readily be converted into methyl methacrylate, the precursor of poly-methyl methacrylate. This compound has a market size of more than 3 million tons per year, as it can be used for the production of acrylic glass, coating materials, and inks (1, 7). Therefore, 2-HIBA has emerged as a target product of biorefinery processes.

As a proof of principle, production of 2-HIBA by *Cupriavidus necator* H16 strains expressing HCM genes has already been demonstrated with fructose, butyric acid, or carbon dioxide plus knallgas as the substrates (8–11). However, product yields were very low in these early studies, an observation that was subsequently ascribed to the fact that HCM from *Aquincola tertiaricarbonis* L108 is highly specific for (*S*)-3-hydroxybutyryl-CoA and thus poorly compatible with the PHB cycle (3). In the search for an (*R*)-3-hydroxybutyryl-CoA-specific coenzyme B_{12}-dependent mutase (RCM), a candidate isolated from the thermophilic knallgas bacterium *Kyrpidia tusciae* DSM 2912 was characterized and could indeed be shown to favor the (*R*)-isomer (12). After the concomitant heterologous expression of the PhaA, PhaB, and RCM genes, the formation of 2-HIBA could be successfully demonstrated in *Escherichia coli* strains, but the final titers did not exceed 70 mg $liter^{-1}$. As the level of production of (*R*)-3-hydroxybutyric acid was much higher in these strains, it was concluded that the thermophilic character of the mutase impedes higher 2-HIBA yields. In this connection, a potentially mesophilic RCM candidate was found in the bacterium *Bacillus massiliosenegalensis* JC6, which was reported to grow well at 37°C (13). This enzyme and the RCM from *K. tusciae* DSM 2912 share 78.2%, 77.4%, and 52.8% sequence identity with the large substrate-binding mutase subunit RcmA, the small coenzyme B_{12}-binding subunit RcmB, and the associated putative G protein chaperone MeaH, respectively (12). Furthermore, the RCM genes are arranged in an identical operonic structure. In the case of strain JC6, it remains to be tested if the putative mutase really shows the expected catalytic properties.

One major disadvantage of most biotechnological production processes is the primary employment of sugar substrates (1), thereby being in a conflict with food and fodder production. More dispensable substrates, for instance, C_1 compounds, such as CO_2, formic acid, and methanol, appear to be promising alternatives. A strong potential has long since been attributed especially to methanol, owing to its physical properties, which make it convenient for handling and transport; a relatively low and stable price; and a potentially sustainable means of production from wood, agricultural waste materials, and biogas (14–16). Furthermore, a variety of microorganisms, referred to as methylotrophs, are able to grow on methanol as the sole source of carbon and energy (17). A well-studied representative is *Methylobacterium extorquens* AM1, a

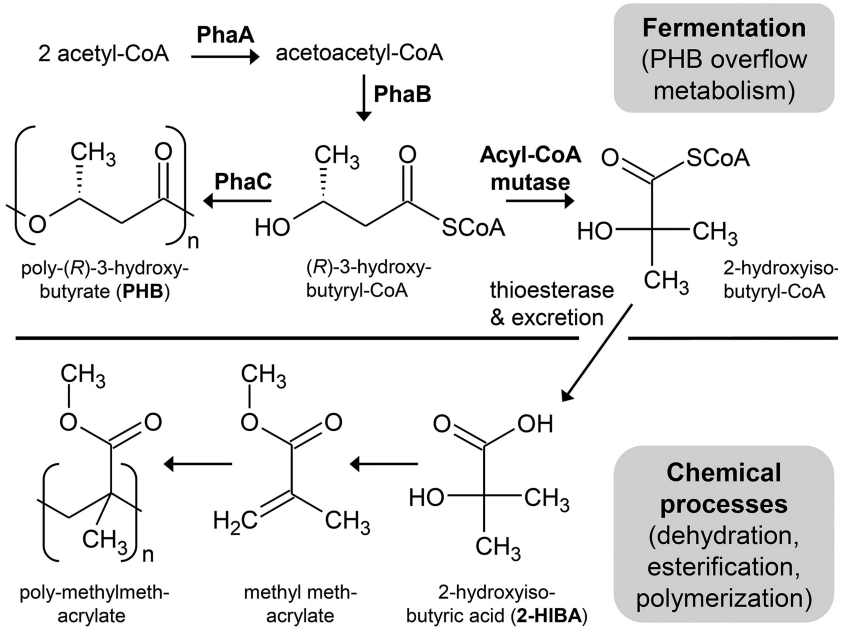

FIG 1 Acyl-CoA mutase-dependent synthesis route for biotechnological production of 2-hydroxyisobutyric acid (2-HIBA) using the polyhydroxybutyrate (PHB) pathway and chemical conversion into poly-methyl methacrylate. PhaA, beta-ketothiolase; PhaB, acetoacetyl-CoA reductase; PhaC, PHB synthase.

pink-pigmented, aerobic alphaproteobacterium first identified in 1961 (18). This model methylotroph has already been applied for the synthesis of industry-relevant products, for example, mevalonic acid, mesaconic acid, and methylsuccinic acid, from methanol (19, 20). The exceptional metabolism of this bacterium was not completely elucidated until recently (21, 22). Aside from the serine cycle used for assimilation of methanol via methylene-tetrahydrofolate, *M. extorquens* AM1 was shown to employ the ethylmalonyl-CoA (EMC) pathway to regenerate metabolic intermediates (23). This includes the reactions of PhaA and PhaB, which overlap the PHB pathway (Fig. 2). (*R*)-3-Hydroxybutyryl-CoA is then transformed over a series of CoA thioester derivatives, requiring the activity of two B_{12}-dependent acyl-CoA mutases (i.e., ethylmalonyl-CoA mutase and methylmalonyl-CoA mutase) and thus the endogenous synthesis of coenzyme B_{12} (24). Due to these metabolic properties, strain AM1 seems to be a suitable candidate for 2-HIBA production via RCM.

In order to establish a biotechnological 2-HIBA production route via the bacterial PHB overflow metabolism, we characterized a putative acyl-CoA mutase from *B. massiliosenegalensis* JC6. Although its biochemical properties are quite similar to those of the thermophilic RCM previously found in strain *K. tusciae* DSM 2912 (12), the new RCM possesses a mesophilic temperature optimum. Both RCM variants could be heterologously expressed in strain *M. extorquens* AM1, allowing the investigation of 2-HIBA production from methanol in controlled fed-batch bioreactor experiments. To evaluate the performance of recombinant strains, fermentation experiments were accompanied by reverse transcription (RT)-quantitative PCR (qPCR) analysis for the RCM genes as well as for various metabolic genes of the dissimilatory and assimilatory pathways of strain AM1.

RESULTS

Kinetic parameters of purified RCM_{Bmas}. After heterologous expression of the putative mutase genes *rcmA* and *rcmB* from strain JC6 in *E. coli* ArcticExpress and purification via affinity chromatography, the molecular weight and purity of the proteins were controlled via sodium dodecyl sulfate-polyacrylamide gel electrophoresis (SDS-PAGE) (see Fig. S1 in the supplemental material). Following the assembly of

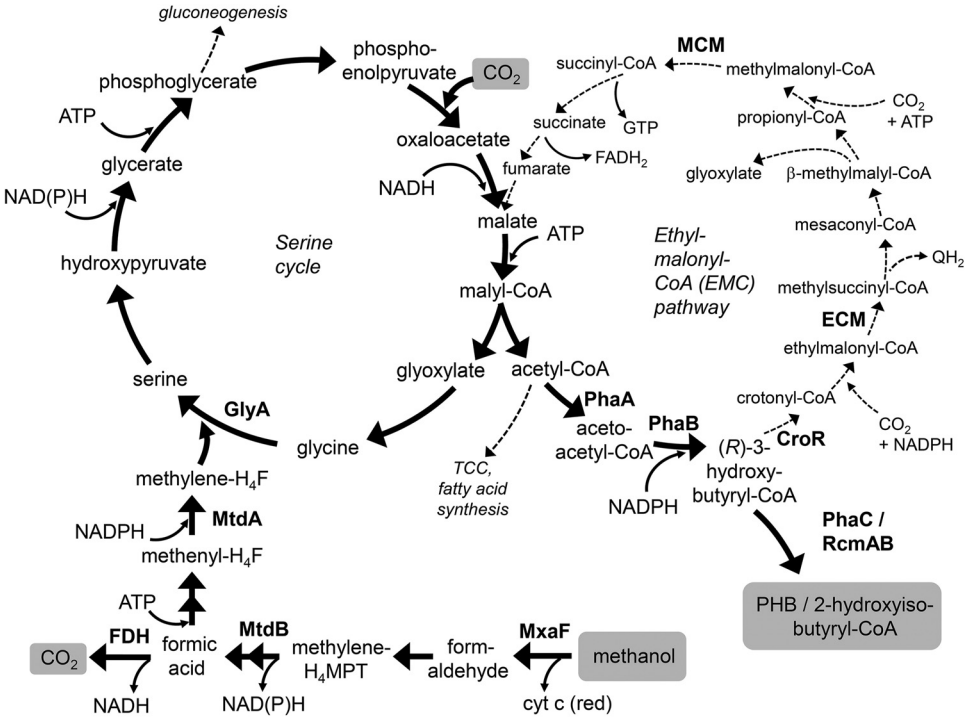

FIG 2 Part of the metabolism of *M. extorquens* AM1, including the oxidation of methanol, the serine cycle, and the ethylmalonyl-CoA (EMC) pathway overlapping the PHB pathway. The conversion of (*R*)-3-hydroxybutyryl-CoA into PHB or 2-hydroxyisobutyryl-CoA by heterologously expressed (*R*)-3-hydroxybutyryl-CoA-specific coenzyme B_{12}-dependent mutase is indicated. MxaF, methanol dehydrogenase; H_4F, tetrahydrofolate; H_4MPT, tetrahydromethanopterin; MtdB, methylene-H_4MPT dehydrogenase; MtdA, methylene-H_4F dehydrogenase; FDH, formate dehydrogenase; GlyA, serine hydroxymethyl transferase; PhaA, beta-ketothiolase; PhaB, acetoacetyl-CoA reductase; CroR, crotonase; ECM, ethylmalonyl-CoA mutase; MCM, methylmalonyl-CoA mutase; PhaC, PHB synthase; RcmAB, (*R*)-3-hydroxybutyryl-CoA-specific mutase; MeaH, G protein chaperone associated with RcmAB; TCC, tricarboxylic acid cycle; QH_2, reduced quinone; cyt c (red), reduced cytochrome *c*.

both subunits in activity assays, the enzyme could be shown to convert the acyl-CoA substrate 2-hydroxyisobutyryl-CoA as well as the substrates (*R*)- and (*S*)-3-hydroxybutyryl-CoA. The pH optimum obtained with 2-hydroxyisobutyryl-CoA was found to be 7.8, equal to that of the RCM of *K. tusciae* DSM 2912 (RCM_{Ktus}) (Fig. S2A). The optimum temperature was 35°C, with the specific activity being reduced by about 40 and 80% at 20 and 50°C, respectively (Fig. S2B). Therefore, the RCM from *B. massiliosenegalensis* JC6 (RCM_{Bmas}) was considered to be mesophilic. Subsequently, the values of the kinetic parameters for all three acyl-CoA substrates were determined at 35°C (Table 1) and compared to the values of the kinetic parameters for RCM_{Ktus} previously obtained at 55°C (12). Likely due to the different thermal adaptation, with the activity being about 220 nmol min^{-1} mg^{-1} for both (*R*)-3-hydroxybutyryl- and

TABLE 1 Kinetic parameters for RCM_{Bmas} and RCM_{Ktus} determined at optimum temperatures[b]

Enzyme	Substrate	V_{max} (nmol min^{-1} mg^{-1})	K_m (μM)	k_{cat} (min^{-1})	k_{cat}/K_m (mM^{-1} min^{-1})
RCM_{Bmas}	(*R*)-3-Hydroxybutyryl-CoA	222 ± 6.1	69 ± 9.9	18 ± 0.5	264 ± 39
	2-Hydroxyisobutyryl-CoA	218 ± 8.3	162 ± 25	18 ± 0.7	111 ± 18
	(*S*)-3-Hydroxybutyryl-CoA	62 ± 1.9	249 ± 28	5.2 ± 0.2	20 ± 2.4
RCM_{Ktus}[a]	(*R*)-3-Hydroxybutyryl-CoA	3,530 ± 40	87 ± 3.0	293 ± 3.3	3,360 ± 135
	2-Hydroxyisobutyryl-CoA	2,640 ± 99	90 ± 13	219 ± 8.2	2,430 ± 361
	(*S*)-3-Hydroxybutyryl-CoA	1,130 ± 78	313 ± 88	94 ± 6.5	300 ± 87

[a]Values were determined previously (12).
[b]The optimum temperatures were 35°C and 55°C for RCM_{Bmas} and RCM_{Ktus}, respectively.

2-hydroxyisobutyryl-CoA and the activity for (*S*)-3-hydroxybutyryl-CoA being more than 3.5-fold lower, the V_{max} values of the mesophilic RCM_{Bmas} were approximately 1 order of magnitude lower than those of RCM_{Ktus}. The K_m values, on the other hand, were in similar ranges between about 70 and 300 μM, and for both enzymes they were equally 3.6 times higher for (*S*)-3-hydroxybutyryl-CoA than for (*R*)-3-hydroxybutyryl-CoA. Accordingly, RCM_{Bmas} and RCM_{Ktus} prefer the (*R*)-enantiomer over the (*S*)-enantiomer with 13- and 11-fold efficiencies, respectively. The values of the kinetic parameters for 2-hydroxyisobutyryl-CoA were between those of the 3-hydroxybutyryl-CoA stereoisomers.

2-HIBA production in *M. extorquens* AM1 transformed with different plasmids. DNA fragments encoding the mutase subunits RcmA and RcmB and the putative G protein chaperone MeaH of *K. tusciae* DSM 2912 and *B. massiliosenegalensis* JC6 were cloned into different expression vectors (see Fig. S3 and the supplemental material for the DNA sequence alignments as well as the codon-optimized sequences in GenBank format). Apart from the original sequence of the three genes of strain DSM 2912 in their operonic order (*meaH-rcmA-rcmB*), two codon-optimized sequences of both strains were generated by replacing rarely used codons of *M. extorquens* and *E. coli*. For heterologous expression, we chose the broad-host-range vector pBBR1MCS-3 carrying a *lac* promoter (25), and pCM80, which was especially designed for methylotrophic strains and contains P_{lac} as well as P_{mxaF}, the promoter of the methanol dehydrogenase gene *mxaF* of strain AM1 (26). The *M. extorquens* AM1 wild-type strain was transformed with the respective pBBR1MCS-3 and pCM80 variants listed in Table 2 and grown on methanol in shaking flasks. All recombinant strains accumulated 2-HIBA at concentrations ranging from 50 to 200 mg liter^{-1} (Fig. 3 and S4), indicating that the RCM genes were successfully expressed from both vector types tested. However, differences in performance could hardly be assigned to either the pCM80 or the pBBRMCS-3 variant or to the usage of codon-optimized or original sequences. Rather, the origin of the RCM genes seemed to be important, as the average final concentrations of 2-HIBA in cultures expressing the RCM_{Bmas} variants were about 2-fold higher than those in cultures expressing the RCM_{Ktus} genes. The highest titers for each RCM variant were obtained with pBBR1MCS-3 $[meaH\text{-}rcmA\text{-}rcmB]_{Bmas\ codon\text{-}optimized}$ and pBBR1MCS-3 $[meaH\text{-}rcmA\text{-}rcmB]_{Ktus\ codon\text{-}optimized}$, reaching concentrations of 230 and 130 mg liter^{-1}, respectively.

Fed-batch bioreactor experiments with recombinant *M. extorquens* AM1. The performance of recombinant AM1 strains was also assessed under more controlled conditions in fed-batch bioreactor experiments. To induce PHB overflow metabolism, the methanol feed was adjusted to maintain excess carbon conditions, while only a limited amount of 5 g liter^{-1} of $(NH_4)_2SO_4$, corresponding to about 1 g liter^{-1} of nitrogen, was supplied. Thus, after complete nitrogen consumption, the cells were expected to produce PHB as well as 2-HIBA. For these experiments, the *M. extorquens* AM1 strains transformed with pBBR1MCS-3 $[meaH\text{-}rcmA\text{-}rcmB]_{Bmas\ codon\text{-}optimized}$ and pBBR1MCS-3 $[meaH\text{-}rcmA\text{-}rcmB]_{Ktus}$ were chosen. Interestingly, cultivation proceeded quite differently (Fig. 4). The RCM_{Bmas} variant grew exponentially for about 50 h and then nearly linearly for another 20 h before maximal biomass concentrations were attained. In contrast, with the RCM_{Ktus} variant, exponential growth was observed only within the first 40 h. Afterwards, the growth rate decreased continuously and maximal biomass values were not reached until 100 h. By analyzing the off-line and online data, i.e., the stirring rate and the amount of base added, the total fermentation process could be roughly divided into a nitrogen-dependent growth phase, a PHB production phase, and a stationary phase (Fig. 4). The complete nitrogen consumption after about 50 and 75 h for the RCM_{Bmas} and RCM_{Ktus} variants, respectively, marked the beginning of the 40- to 50-h lasting PHB production phase, subsequently followed by the stationary phase. Finally, after a total time span of 7 and 8 days for the RCM_{Bmas} and RCM_{Ktus} variants, respectively, the biomass concentrations started to decline and the experiments were terminated.

TABLE 2 Bacterial strains, plasmids, and primers used in this study

Strain, plasmid, or primer	Characteristics or sequence	Reference or source
Strains		
E. coli ArcticExpress (DE3)	F$^-$ *ompT hsdS*$_B$(r_B^- m_B^-) *dcm* Tet^r *gal endA hte* [*cpn10 cpn60* Gent^r] λ(DE3)	Agilent
Methylobacterium extorquens AM1	DSM 1338, wild type	DSMZ
Plasmids		
pBBR1MCS-3	Expression vector, P_{lac} Tet^r	25
pCM80	Expression vector, P_{lac} P_{mxaF} Tet^r	26
pASG-IBA43	Expression vector, *tetA* promoter, Amp^r	IBA, Goettingen, Germany
pET-16b	Expression vector, T7 promoter, Amp^r	Novagen
pBBR1MCS-3 [meaH-rcmA-rcmB]$_{Ktus}$	*meaH-rcmA-rcmB* from *K. tusciae* DSM 2912 inserted into pBBR1MCS-3	12
pBBR1MCS-3 [meaH-rcmA-rcmB]$_{Ktus\ codon\text{-}optimized}$	*meaH-rcmA-rcmB* from *K. tusciae* DSM 2912 generated via gene synthesis and inserted into pBBR1MCS-3	This study
pBBR1MCS-3 [meaH-rcmA-rcmB]$_{Bmas\ codon\text{-}optimized}$	*meaH-rcmA-rcmB* from *B. massiliosenegalensis* JC6 generated via gene synthesis and inserted into pBBR1MCS-3	This study
pCM80 [meaH-rcmA-rcmB]$_{Ktus}$	*meaH-rcmA-rcmB* from *K. tusciae* DSM 2912 inserted into pCM80	This study
pCM80 [meaH-rcmA-rcmB]$_{Ktus\ codon\text{-}optimized}$	*meaH-rcmA-rcmB* from *K. tusciae* DSM 2912 generated via gene synthesis and inserted into pCM80	This study
pCM80 [meaH-rcmA-rcmB]$_{Bmas\ codon\text{-}optimized}$	*meaH-rcmA-rcmB* from *B. massiliosenegalensis* JC6 generated via gene synthesis and inserted into pCM80	This study
pASG-IBA43 [rcmA]$_{Bmas\ codon\text{-}optimized}$	*rcmA* from pBBR1MCS-3 [meaH-rcmA-rcmB]$_{Bmas\ codon\text{-}optimized}$ inserted into pASG-IBA43	This study
pET-16b [rcmB]$_{Bmas\ codon\text{-}optimized}$	*rcmB* from pBBR1MCS-3 [meaH-rcmA-rcmB]$_{Bmas\ codon\text{-}optimized}$ inserted into pET-16b	This study
Primers		
rcmA_Bmas_f	5′-AGC GGC TCT TCA ATG ACC AAG GCT AAC GTG AAC-3′	This study
rcmA_Bmas_r	5′-AGC GGC TCT TCT CCC CGC GAG CGG GAA CTG CC-3′	This study
NdeI_rcmB_Bmas_f	5′-ATA TCA TAT GCA GGT CAA GGT GGT CAT G-3′	This study
BamHI_rcmB_Bmas_r	5′-ATA TGG ATC CTT ACC CGA TCT TCT TCC CCA C-3′	This study
q_mxaF_Mex_f	5′-CGA CTT GAA CAC GTT GAC CG-3′	This study
q_mxaF_Mex_r	5′-GAA GCC AAG TTC GGC TAC CA-3′	This study
q_glyA_Mex_f	5′-GAG ATC GAG CTG ATC GCG T-3′	This study
q_glyA_Mex_r	5′-CTG AAT TCG GCT GCA CGT TG-3′	This study
q_phaB_Mex_f	5′-ATT ACG GCG GAA ACG ACG AG-3′	This study
q_phaB_Mex_r	5′-ATC GAG TCG AGG TTG GTG C-3′	This study
q_croR_Mex_f	5′-GAT CGC AAC CCG ATC CAC C-3′	This study
q_croR_Mex_r	5′-CCT CGA CCT TCA CCT CGA C-3′	This study
q_recA_Mex_f	5′-GTT CTT GAC GAC CTT GAC GC-3′	This study
q_recA_Mex_r	5′-AAG CTC ACC GGT TCG ATC TC-3′	This study
q_rpoD_Mex_f	5′-GGT TGG TGT ACT TCT TGG CG-3′	This study
q_rpoD_Mex_r	5′-GGA AGA ACT TCG TGG AGC GT-3′	This study
q_meaH_Ktus_f	5′-CCG CAA AAC TCT CCA AAC GG-3′	This study
q_meaH_Ktus_r	5′-CAC TTC TTT CCC GTA GGC GT-3′	This study
q_rcmA_Ktus_f	5′-GGA TTC GGA ACT CCG GAA GA-3′	This study
q_rcmA_Ktus_r	5′-CTG ATC GAT GGG GAT TCC GT-3′	This study
q_rcmB_Ktus_f	5′-TGT TCC CCG AAC AGA TCG TC-3′	This study
q_rcmB_Ktus_r	5′-CGA ACA CTT CAG CGA TTC CC-3′	This study
q_meaH_Bmas_f	5′-CGA CGA GCA TCG AAA TCC TG-3′	This study
q_meaH_Bmas_r	5′-ACA CAT TCG ACA GAC CCG AC-3′	This study
q_rcmA_Bmas_f	5′-GGA TAT GGA ACG CCG GAA GA-3′	This study
q_rcmA_Bmas_r	5′-CGG GAT CCC ATC ATA AAG CG-3′	This study
q_rcmB_Bmas_f	5′-TTC CCG GAA CAG ATC GTG G-3′	This study
q_rcmB_Bmas_r	5′-CGA ACA CTT CAG CGA TTC CG-3′	This study

To compare the different performance characteristics of the two culture variants in more detail, the specific growth and product formation rates and the maximal product concentrations as well as the respective yields from methanol were calculated (Table 3). These data clearly show that the RCM_{Ktus} culture was severely inhibited. Only the specific growth rates in the exponential phase were quite similar for both strains tested. The corresponding maximal biomass yields, however, were already 1.7-fold lower in the RCM_{Ktus} variant, and maximal biomass and PHB values, reached after the PHB produc-

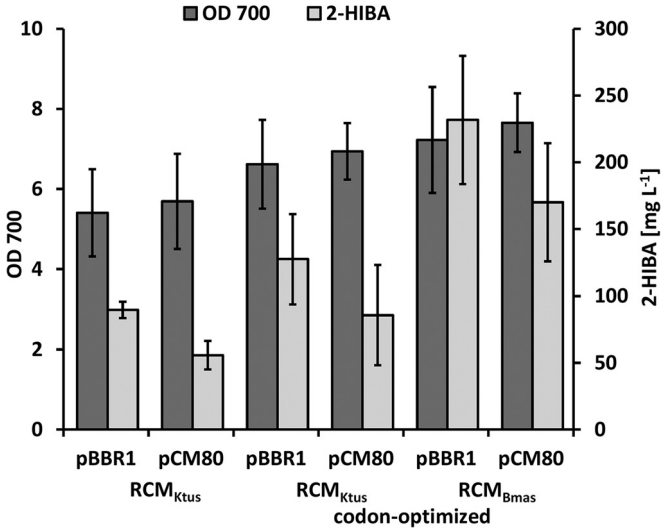

FIG 3 Shaking-flask experiments for testing the growth and product formation of *M. extorquens* AM1 strains transformed with different expression vectors and RCM gene clusters. Final optical density values and 2-hydroxyisobutyric acid titers after 7 days of incubation are shown. Data represent mean values and standard deviations from at least four independent experiments (see also Fig. S4 in the supplemental material). OD 700, optical density measured at 700 nm as an indicator of biomass increase; 2-HIBA, 2-hydroxyisobutyric acid concentration in culture supernatant; pBBR1, expression vector pBBR1MCS-3; pCM80, expression vector pCM80; RCM_{Ktus}, vector insert $[meaH\text{-}rcmA\text{-}rcmB]_{Ktus}$; RCM_{Ktus} codon optimized, vector insert $[meaH\text{-}rcmA\text{-}rcmB]_{Ktus}$ with a codon-optimized sequence; RCM_{Bmas} codon optimized, vector insert $[meaH\text{-}rcmA\text{-}rcmB]_{Bmas}$ with a codon-optimized sequence.

tion phase, were even reduced 2.5- and 3-fold, respectively. Likewise, final 2-HIBA titers of about 2.1 g liter^{-1} were obtained with the RCM_{Bmas} variant, corresponding to an amount 5-fold larger than that produced by the AM1 strain expressing the RCM_{Ktus} genes. In addition, the better performance of the RCM_{Bmas} variant became obvious from all other parameters calculated, such as total biomass and product yields and maximal product formation rates (Table 3). With values of 0.087 and 0.027 g g^{-1}, respectively, the best PHB and 2-HIBA yields were obtained in the PHB production phase directly after complete nitrogen consumption. This means that about 24% of the methanol channeled to the PHB overflow metabolism could be converted into 2-HIBA.

RCM activity in recombinant *M. extorquens* AM1. To elucidate the differences in growth and 2-HIBA production of the recombinant *M. extorquens* AM1 strains studied in the fed-batch bioreactor experiments, the specific RCM activities in crude extracts from fermentation samples taken at different time intervals were determined. The respective enzyme assays were not performed at the optimum temperatures of the mutases but were performed at the cultivation temperature of 30°C. Thereby, the specific activities of RCM_{Bmas} were observed to be substantially higher than those of RCM_{Ktus} (Fig. 5). The maximum value (20.7 nmol min^{-1} mg^{-1}) was even twice as high (9.7 nmol min^{-1} mg^{-1}), and a shift with time could be detected. The specific activity of RCM_{Bmas} was already quite high at 48 h and increased to its maximal value at 72 h before it started to decline. RCM_{Ktus}, on the other hand, showed a slight increase from 48 h to 72 h, reached a maximum at 96 h, and subsequently decreased. This behavior corresponds to the generally slower growth of *M. extorquens* AM1 expressing RCM_{Ktus} genes (Fig. 4). However, both strains equally exhibited the highest specific activity within the PHB production phase, and during stationary phase, the activities decreased to about 50% of the maximal value.

Expression of metabolic and RCM genes in recombinant *M. extorquens* AM1. In addition to the investigations described above, an expression analysis via RT-qPCR was expected to deliver valuable information concerning overflow metabolism and 2-HIBA production in recombinant *M. extorquens* AM1. Therefore, not only the RCM genes but also genes of key enzymes involved in the metabolism of *M. extorquens* (Fig. 2) were

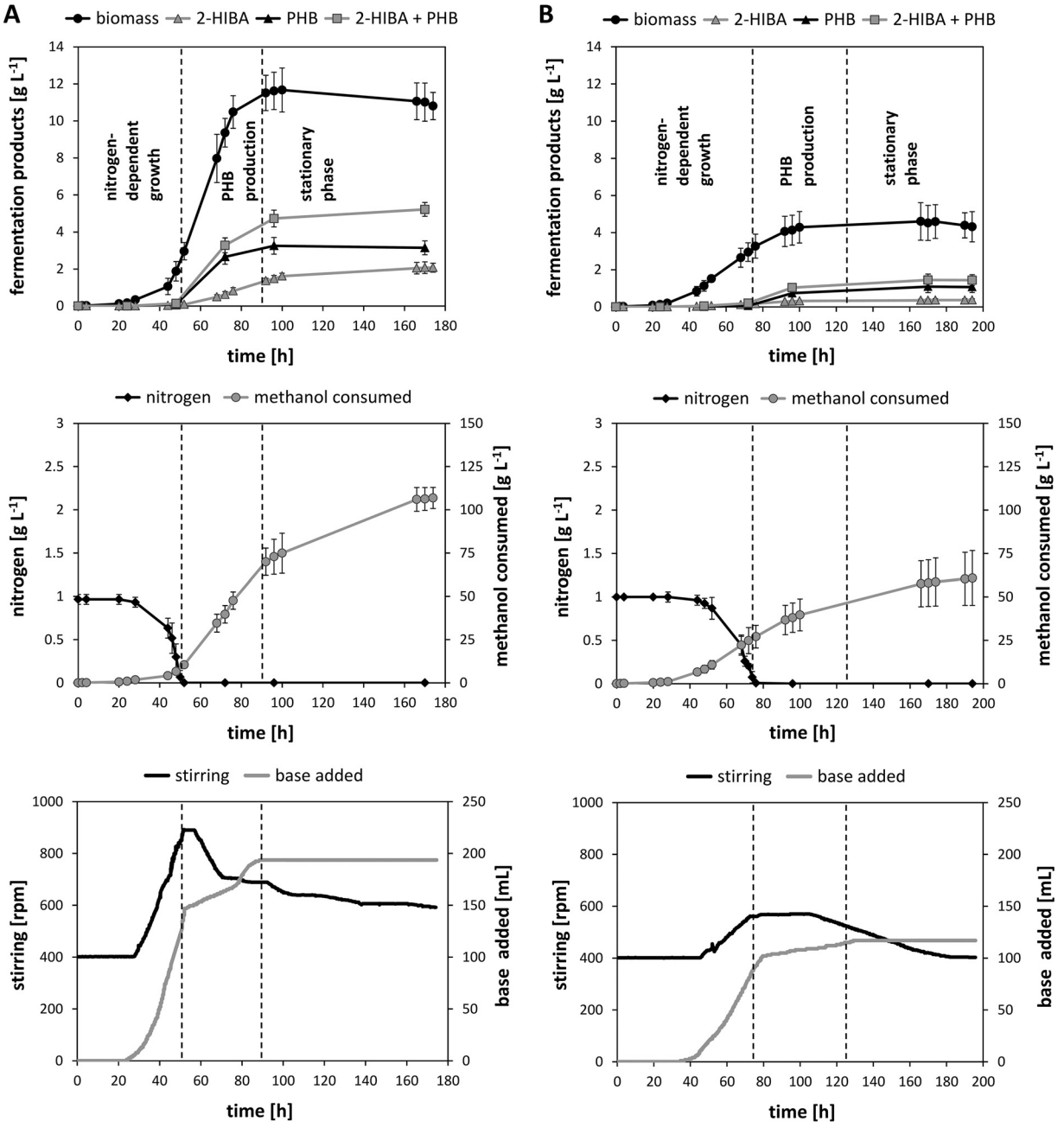

FIG 4 Course of fed-batch bioreactor experiments of *M. extorquens* AM1 transformed with pBBR1MCS-3 [meaH-rcmA-rcmB]$_{\text{Bmas codon-optimized}}$ (A) and pBBR1MCS-3 [meaH-rcmA-rcmB]$_{\text{Ktus}}$ (B). The concentrations of biomass, 2-HIBA, PHB, and nitrogen were determined from fermentation samples, as indicated, and the amount of cumulative methanol consumption was calculated from the amount of methanol added and the residual methanol concentration within each sample. Online data for the stirring rate and the amount of base added during fermentation are shown exemplarily for single experiments. All other data represent values and standard deviations from at least three independent experiments. The different phases of the fermentations (nitrogen-dependent growth, PHB production phase, stationary phase) are indicated.

considered. As such, we chose the genes for the methanol dehydrogenase (*mxaF*), the serine hydroxymethyl transferase (*glyA*), the acetoacetyl-CoA reductase (*phaB*), and the crotonase (*croR*). Additionally, two reference genes encoding recombinase A (*recA*) and the RNA polymerase sigma factor (*rpoD*) were applied for relative quantification of the qPCR data. Respective primers for the target and reference genes yielding PCR fragments of 200 to 250 bp in size were designed (Table 2). For RT-qPCR, whole cellular RNA from fermentation samples of *M. extorquens* AM1 transformed with the RCM$_{\text{Bmas}}$ or RCM$_{\text{Ktus}}$ genes was isolated, and the first samples taken after 24 h were chosen as a

TABLE 3 Fermentation product concentrations, formation rates, and yields of *M. extorquens* AM1 expressing different RCM variants[a]

Characteristic	Value for:	
	RCM_{Bmas}	RCM_{Ktus}
Maximum specific growth rate (h^{-1})	0.139 ± 0.010	0.131 ± 0.011
Maximum biomass yield (g g^{-1})	0.317 ± 0.059	0.192 ± 0.017
Maximum biomass concn (g $liter^{-1}$)	11.67 ± 1.20	4.60 ± 1.01
Maximum PHB concn (g $liter^{-1}$)	3.25 ± 0.45	1.09 ± 0.32
Maximum 2-HIBA concn (g $liter^{-1}$)	2.07 ± 0.32	0.37 ± 0.07
Total biomass yield (g g^{-1})	0.109 ± 0.008	0.076 ± 0.007
Total PHB yield (g g^{-1})	0.045 ± 0.004	0.019 ± 0.003
Total 2-HIBA yield (g g^{-1})	0.022 ± 0.003	0.006 ± 0.001
Maximum PHB formation rate (g $liter^{-1}$ h^{-1})	0.168 ± 0.030	0.032 ± 0.005
Maximum 2-HIBA formation rate (g $liter^{-1}$ h^{-1})	0.037 ± 0.002	0.008 ± 0.002
PHB yield, PHB production phase (g g^{-1})	0.087 ± 0.004	0.025 ± 0.002
2-HIBA yield, PHB production phase (g g^{-1})	0.027 ± 0.001	0.007 ± 0.001
Yield of 2-HIBA + PHB, PHB production phase (g g^{-1})	0.114 ± 0.004	0.032 ± 0.002

[a]Total yields (per methanol molecule consumed) were determined when strains attained the highest biomass concentrations, i.e., after 4 days in the case of RCM_{Bmas} and after 7 days in the case of RCM_{Ktus}. Values are means and standard deviations from at least three independent experiments.

control, which was given a value of 1 and to which the level of expression of each gene was normalized to provide an expression ratio (Fig. 6). Compared to the regulation of genes in these samples acquired during exponential growth, only a few genes were upregulated within the following fermentation phases. Instead, with an increase in cultivation time, the majority of target genes showed a decrease in the expression ratio. Especially in the case of RCM_{Bmas}, the expression of *mxaF*, *glyA*, *phaB*, and *croR* declined strongly after complete nitrogen consumption at 52 h. The most severe decrease affected *phaB*, whose expression ratio dropped to 0.02 after 96 h and 170 h. *meaH*, *rcmA*, and *rcmB*, on the other hand, showed an up to 4.8-fold increase in expression ratio within the PHB production phase from 52 h to 72 h. However, during stationary phase, the expression ratios of these genes also decreased about 2- to 5-fold, similar to the expression ratios of the metabolic genes of *M. extorquens*. The expression results for RCM_{Ktus} looked slightly different. Here again it became very obvious that the PHB production phase was delayed by about 24 h. At 48 h as well as at 68 h, the expression ratio of all target genes was quite similar to that for the first sample. After nitrogen consumption at 76 h, the metabolic genes of *M. extorquens* seemed to be downregulated, whereas the expression ratios of *meaH*, *rcmA*, and *rcmB* increased up to 2-fold.

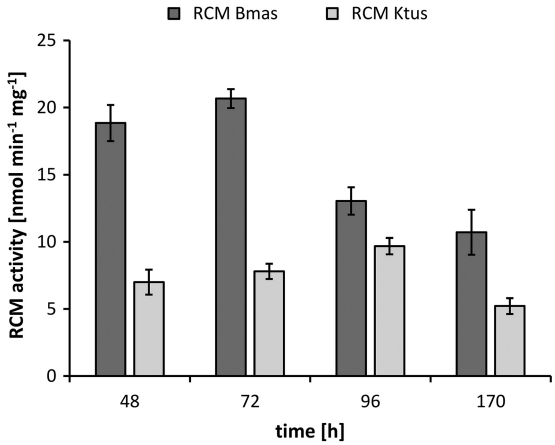

FIG 5 RCM activity determined in crude extracts from samples taken at different time points during fermentation of *M. extorquens* AM1 transformed with pBBR1MCS-3 $[meaH\text{-}rcmA\text{-}rcmB]_{Bmas\ codon\text{-}optimized}$ (RCM Bmas) and pBBR1MCS-3 $[meaH\text{-}rcmA\text{-}rcmB]_{Ktus}$ (RCM Ktus). Mutase assays were conducted at pH 7.8 and 30°C by applying 200 μM (*R*)-3-hydroxybutyryl-CoA as the substrate and a protein concentration of 0.4 mg ml^{-1}. Mean values and standard deviations from three independent experiments are shown.

A

gene \ time	24 h	44 h	52 h	72 h	96 h	170 h
mxaF	1.00	2.07	0.42	0.26	0.12	0.34
glyA	1.00	1.05	0.27	0.25	0.13	0.22
phaB	1.00	0.84	0.14	0.06	0.02	0.02
croR	1.00	1.46	0.57	0.34	0.27	0.35
rcmA	1.00	0.76	2.36	2.49	0.34	0.19
rcmB	1.00	0.66	4.82	3.77	0.52	0.55
meaH	1.00	0.70	2.17	1.64	0.36	0.27

B

gene \ time	24 h	48 h	68 h	76 h	96 h	170 h
mxaF	1.00	0.84	1.39	1.73	0.13	0.09
glyA	1.00	0.86	1.02	0.55	0.18	0.15
phaB	1.00	1.00	1.39	0.99	0.09	0.07
croR	1.00	0.85	0.61	0.51	0.22	0.25
rcmA	1.00	0.83	1.25	0.93	1.02	0.81
rcmB	1.00	0.90	1.04	1.08	2.02	1.49
meaH	1.00	0.81	0.72	1.85	2.04	0.54

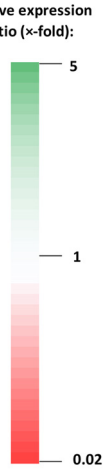

FIG 6 RT-qPCR results for *M. extorquens* AM1 transformed with pBBR1MCS-3 [meaH-rcmA-rcmB]$_{Bmas\ codon\text{-}optimized}$ (A) and pBBR1MCS-3 [meaH-rcmA-rcmB]$_{Ktus}$ (B). For qPCR analysis, total cellular RNA from fermentation samples was isolated and transcribed into cDNA. The given values indicate the relative ratio of expression of the respective gene with reference to that in the first fermentation sample taken after 24 h. Data represent mean values from three independent experiments.

phaB again showed the strongest decline, with an expression ratio of 0.07 after 170 h. All in all, these data give an interesting insight into the gene expression of strain AM1 during cultivation on methanol as well as under conditions of nitrogen limitation. During fermentation, the absolute numbers of *rcm* transcripts of the RCM$_{Bmas}$ or RCM$_{Ktus}$ genes did not change notably and were in the same range (Fig. S5), indicating constitutive expression from the pBBR1MCS-3 vectors that was equally strong in both variants.

DISCUSSION

In the search for suitable mutases for the production of the building block chemical 2-HIBA via the PHB precursor (*R*)-3-hydroxybutyryl-CoA, we characterized a predicted B_{12}-dependent mutase from *B. massiliosenegalensis* JC6 as a mesophilic RCM closely related to the thermophilic mutase from *K. tusciae* DSM 2912. Despite the conserved biochemical properties of both enzymes and although identical vector systems and fermentation conditions were used, heterologous expression of the corresponding RCM$_{Bmas}$ and RCM$_{Ktus}$ genes in *M. extorquens* AM1 on methanol led to substantially different biomass yields and 2-HIBA titers of about 2.1 and 0.4 g liter^{-1}, respectively, suggesting that RCM$_{Bmas}$ is more compatible with the metabolism of this strain.

As already proposed from sequence analysis classifying it as an RCM-like enzyme (12), the newly characterized mutase from strain JC6 catalyzes the isomerization of 2-hydroxyisobutyryl- and 3-hydroxybutyryl-CoA esters with catalytic efficiency ratios in the same range as those previously found for the RCM from the thermophilic strain DSM 2912. Consequently, both enzymes equally favor the (*R*)-enantiomer above the (*S*)-enantiomer of 3-hydroxybutyryl-CoA. Nevertheless, we clearly characterized RCM$_{Bmas}$ as a mesophilic enzyme showing a temperature optimum of 35°C, while RCM$_{Ktus}$ has its activity maximum at 55°C (12). This thermal adaptation may be caused by various molecular mechanisms, such as the number of salt bridges and hydrophobic interactions (27). In particular, the flexibility of surface-exposed loops may be crucial, as has been recently demonstrated for esterases with conserved biochemical properties but substantially different temperature optima (28). However, without structure models for the RCM enzymes precisely describing the position and interaction of all loops and other structure elements and due to the lack of general models for the prediction of the thermal stability of proteins (28), we are currently not able to explain the observed differences.

By introducing the RCM genes into *M. extorquens* AM1, the production of 2-HIBA from methanol could be demonstrated with both broad-host-range expression vector systems, pCM80 and pBBR1MCS-3, under P_{mxaF} and P_{lac} control, respectively. Obviously, although it has been reported several times that heterologous expression in *M. extorquens* strains is much stronger when it is controlled by P_{mxaF} than when it is controlled by P_{lac} (26, 29–31), the transcript levels of the RCM genes in all recombinant strains were sufficiently high to generate substantial RCM activities in our case. More importantly, transformation with pBBR1MCS-3 resulted in slightly higher 2-HIBA titers than transformation with the pCM80 expression system. This clearly demonstrates that not only transcription but also posttranscriptional processes, such as translation, protein folding, and cofactor binding, may be critical for creating a heterologous function. In line with this, it has recently been shown that both P_{mxaF}- and P_{lac}-controlled expression of the alcohol dehydrogenase AdhE2 gene from *Clostridium acetobutylicum* in strain AM1 resulted in nearly identical corresponding butanol and butyraldehyde oxidation rates (32). Consequently, for each new metabolic gene, not only expression levels but also enzyme activities and the impact on fitness have to be tested. Therefore, besides P_{mxaF} and P_{lac}, a couple of other promoters with different strengths are already available for heterologous expression in strain AM1 (32, 33). In addition, inducible vectors allowing titratable activation of promoters have been developed (34).

In order to study the performance of the different RCM enzymes in more detail, we chose the strains expressing either the RCM_{Ktus} or RCM_{Bmas} genes via the pBBR1MCS-3 vector for fed-batch bioreactor experiments, allowing strict control of the fermentation conditions and nutrient supply. As expected, with both strains the highest rates of 2-HIBA production were achieved within the PHB production phase. However, with cells expressing the RCM_{Ktus} gene, metabolic activity was substantially inhibited, leading to up to 3-fold reduced final amounts of biomass and PHB compared to those achieved with the RCM_{Bmas} variant. More seriously, RCM activities were likewise affected, resulting in substantially lower 2-HIBA titers. Under similar cultivation conditions (with 1 g liter^{-1} nitrogen as ammonia in the medium), we routinely obtained about 15 to 17 g liter^{-1} biomass and cellular PHB and nitrogen contents close to 37% and 6%, respectively, with wild-type strain AM1 (35). This indicates that the RCM_{Bmas} variant already shows slight growth inhibition, resulting in maximal biomass values of only 12 g liter^{-1} and deduced cellular nitrogen values of about 8%. Obviously, in both recombinant strains the ability to adapt to nitrogen limitation by PHB production and recycling of cellular components, e.g., by ribophagy (36), is substantially decreased.

Generally, heterologous expression could represent a substantial metabolic burden for the host (37), and several measures, such as antibiotic-free plasmid maintenance and tuning of expression levels, have been proposed to mitigate this effect (38). However, as both engineered strains possess identical expression vectors with similar insert lengths (3,141 and 3,084 bp for the RCM_{Bmas} and RCM_{Ktus} variants, respectively) and were incubated under the same conditions, the remarkably low growth and product yields of the RCM_{Ktus} culture are somewhat surprising. The inhibitory effect seems to be rather caused directly by the heterologous proteins. However, neither in the RCM_{Bmas} nor in the RCM_{Ktus} variant were we able to detect abnormal protein aggregates via SDS-PAGE (data not shown). In addition, a toxicity of the mutase proteins has not been previously observed when the RCM_{Ktus} genes are expressed in *E. coli* BL21 via the pBBR1MCS-3 vector (12). Likewise, similar inhibitory effects of heterologous proteins have not been reported in most studies on recombinant AM1 (26, 32, 39–41) or other *M. extorquens* strains (29–31). In contrast, Chou and coworkers (42) found that rates of expression of a nonorthologous formaldehyde oxidation pathway in strain AM1 that were too high led to a growth rate that was one-third that of the wild type. In addition, the physiological problems caused by overexpression resulted in cells of increased length and aberrant morphology. However, as the expression levels of RCM genes were quite similar for both variants and the cells did not show any aberrant morphology (see Fig. S5 and S6 in the supplemental material), the reduced metabolic activity observed in our case was

obviously not related to a typical protein expression burden. In summary, although we do not yet have any conclusive explanation, our results indicate that the RCM proteins from strain JC6 seem to be more compatible with AM1 metabolism, suggesting that already closely related protein variants might have substantially different effects on metabolic activity when heterologously expressed.

Subsequent to nitrogen consumption, in both cultures the levels of transcription of genes encoding several key enzymes of AM1 metabolism, i.e., MxaF, GlyA, PhaB, and CroR (Fig. 2), strongly decreased within the PHB production and stationary phases. Depending on protein turnover rates, the lower levels of expression will affect corresponding enzyme activities and downregulate the whole metabolism in the end. Most importantly for 2-HIBA production, provision of (*R*)-3-hydroxybutyryl-CoA as the substrate for PhaC and RCM was likely steadily reduced while cultivation continued. In line with this, PHB was not produced anymore in the stationary phase, and although the expression of the RCM genes was kept at levels higher than the levels of expression of the above-mentioned metabolic genes, only small amounts of 2-HIBA were still produced at that time. This restriction is apparently not due to cellular limitations, as the PHB content did not exceed 29%, which is clearly below the maximal values of up to 42% attained with the AM1 wild type (43). Rather, there must be a yet unknown mechanism of regulation resulting in a time-dependent termination of the overflow metabolism, likely on both the transcript and enzyme levels. Thus far, investigation of gene and protein levels in AM1 has focused on changes in the central pathways during shifts from methylotrophic and nonmethylotrophic conditions (44, 45). For the development of biotechnological processes, however, future work should also consider transcriptomes and proteomes at different physiological states, such as exponential and stationary growth phases.

Among *M. extorquens* strains, the highest PHB content and yield on methanol have not been achieved with strain AM1 but have been achieved with strain K (deposited as FERM BP-3548 in the International Patent Organism Depositary [IPOD], Japan), reaching values of 60% and 0.2 g g^{-1}, respectively (46). This indicates that a better performance might already be achievable with other strains transformed with RCM_{Bmas}. Furthermore, avoidance of the competing PhaC reaction should also raise 2-HIBA yields. However, previously generated *phaC* knockout mutants of AM1 showed reduced growth and proved to be highly unstable (20, 43), indicating that a certain flux of acetyl-CoA to PHB is essential for efficient metabolism in this bacterium. A convenient solution might be to directly replace *phaC* by the RCM genes, thus avoiding any imbalances due to acetyl-CoA accumulation. Additionally, substrate fluxes to (*R*)-3-hydroxybutyryl-CoA should be optimized by overexpression of *phaAB*, as this has already been shown to enhance the polyhydroxyalkanoate content in AM1 (41) and might extend the overall production phase.

The discovery of RCM enzymes opens the path for employing the PHB overflow metabolism to biotechnologically produce the methyl methacrylate precursor 2-HIBA. Alternatively, methyl methacrylate can be synthesized from biologically based itaconic acid (1). Although the latter process has been intensively developed in the last few years and relatively high titers of up to 80 g $liter^{-1}$ itaconic acid have been achieved using *Aspergillus terreus* strains (47), it is still not commercialized (1). One reason for this is the high substrate cost, as the process is exclusively based on glucose and a few other carbohydrates. In contrast, the mutase route can be established with practically any metabolizable carbon. Here, we propose methanol as the feedstock and the serine cycle as the assimilatory route, as it directly yields the 3-hydroxybutyryl-CoA precursor acetyl-CoA (Fig. 2). Moreover, other C_1 compounds may be applied, as the same metabolism is found in many methanotrophs and is used for assimilating formic acid (17, 48). Basically, all C_1 substrates are available from renewable nonfood resources, e.g., directly from biogas or the electrochemical reduction of CO_2 (49). Interestingly, as the latter technology is highly efficient, a so-called formate-based economy has recently been proposed in which industrial chemicals and fuels are synthesized by forma-

totrophic microorganisms (50). However, substantial progress is still needed to increase the efficiency of C_1 assimilation routes (50, 51).

MATERIALS AND METHODS

Chemicals, bacterial strains, and growth media. All chemicals were of analytical or high-performance liquid chromatography (HPLC) grade and purchased from T. Geyer (Renningen, Germany). 2-Hydroxyisobutyryl-CoA, (*R*)-3-hydroxybutyryl-CoA, and (*S*)-3-hydroxybutyryl-CoA were synthesized from the corresponding free carboxylic acids and CoA via thiophenyl esters as described before (52). The bacterial strains, plasmids, and primers used in this study are listed in Table 2. Cultures of *E. coli* ArcticExpress (DE3) were grown at 30°C in Luria-Bertani broth containing 20 mg liter^{-1} of gentamicin. *M. extorquens* AM1 was cultivated at 30°C in mineral salt medium (53) supplemented with 3 g liter^{-1} of methanol. For bioreactor experiments, increased mineral salt concentrations were used, as follows: $(NH_4)_2SO_4$, 5 g liter^{-1}; KH_2PO_4, 1.305 g liter^{-1}; $Na_2HPO_4{\cdot}7H_2O$, 4.02 g liter^{-1}; $MgSO_4{\cdot}7H_2O$, 0.45 g liter^{-1}; $CaCl_2{\cdot}2H_2O$, 20 mg liter^{-1}; $FeSO_4{\cdot}7H_2O$, 2.6 mg liter^{-1}; $MnSO_4{\cdot}H_2O$, 200 μg liter^{-1}; $ZnSO_4{\cdot}7H_2O$, 260 μg liter^{-1}; $CuSO_4{\cdot}5H_2O$, 80 μg liter^{-1}; $Na_2MoO_4{\cdot}2H_2O$, 80 μg liter^{-1}; $CoCl_2{\cdot}6H_2O$, 80 μg liter^{-1}; and H_3BO_3, 60 μg liter^{-1}. Bacterial growth was monitored by measuring the optical density at 700 nm.

Cloning of RCM genes into expression vectors. Ensuing from the gene sequences of *meaH*, *rcmA*, and *rcmB* from *B. massiliosenegalensis* JC6 (BMSHG_RS03130, BMSHG_RS03125, and BMSHG_RS03120, respectively) and *K. tusciae* DSM 2912 (BTUS_RS02365, BTUS_RS02370, and BTUS_RS02375, respectively), two DNA fragments containing the three genes with codons optimized for expression in *E. coli* and *M. extorquens* AM1 were generated via gene synthesis (GenScript, Piscataway, NJ, USA). Both fragments contained flanking restriction sites for SpeI and SacI, which were used for cloning into the expression vectors pBBR1MCS-3 (25) and pCM80 (26). The complete sequences of both codon-optimized RCM gene clusters are given in the supplemental material. Additionally, the original sequences of the *meaH*, *rcmA*, and *rcmB* genes from strain DSM 2912 were cloned via SpeI and SacI from pBBR1MCS-3 [meaH-rcmA-rcmB]$_{Ktus}$ (12) into pCM80. Subsequently, electrocompetent cells of *M. extorquens* AM1 were transformed with either pBBR1MCS-3 [meaH-rcmA-rcmB]$_{Bmas\ codon\text{-}optimized}$, pCM80 [meaH-rcmA-rcmB]$_{Bmas\ codon\text{-}optimized}$, pBBR1MCS-3 [meaH-rcmA-rcmB]$_{Ktus\ codon\text{-}optimized}$, pCM80 [meaH-rcmA-rcmB]$_{Ktus\ codon\text{-}optimized}$, pBBR1MCS-3 [meaH-rcmA-rcmB]$_{Ktus}$, or pCM80 [meaH-rcmA-rcmB]$_{Ktus}$ via electroporation as described before (29). Colonies carrying the respective plasmids were selected via tetracycline resistance on methanol mineral salt agar plates. For individual expression of RCM genes from strain JC6, DNA fragments encoding *rcmA* and *rcmB* were amplified from pBBR1MCS-3 [meaH-rcmA-rcmB]$_{Bmas\ codon\text{-}optimized}$ via Q5 high-fidelity DNA polymerase (NEB) using forward primer rcmA_Bmas_f and reverse primer rcmA_Bmas_r for *rcmA* and forward primer NdeI_rcmB_Bmas_f and reverse primer BamHI_rcmB_Bmas_r for *rcmB*. The PCR program included 30 cycles of incubation at 94°C for 30 s, 60°C for 30 s, and 72°C for 2 min. Following PCR, the *rcmA* fragment was cloned into pASG-IBA43 according to the protocol of IBA, Goettingen, Germany. The *rcmB* fragment was introduced into pET-16b via the NdeI and BamHI restriction sites. Then, chemocompetent cells of *E. coli* ArcticExpress (DE3) were transformed with either pASG-IBA43 [rcmA]$_{Bmas\ codon\text{-}optimized}$ or pET-16b [rcmB]$_{Bmas\ codon\text{-}optimized}$.

Heterologous expression of *rcmA*$_{Bmas}$ and *rcmB*$_{Bmas}$ in *E. coli* and protein purification. Heterologous RCM subunits A and B were purified via immobilized metal ion affinity chromatography using their N-terminal His tags expressed by pASG-IBA43 and pET-16b. Therefore, *E. coli* ArcticExpress (DE3) strains carrying the expression vectors pASG-IBA43 [rcmA]$_{Bmas}$ and pET-16b [rcmB]$_{Bmas}$ were cultivated in Luria-Bertani broth additionally supplemented with 100 mg liter^{-1} of ampicillin at 30°C at 200 rpm until reaching an optical density of 0.8. Expression of heterologous genes was induced by adding anhydrotetracycline to a final concentration of 0.2 mg liter^{-1} in the case of pASG-IBA43 [rcmA]$_{Bmas}$ and IPTG (isopropyl-β-D-thiogalactopyranoside) to 1 mM in the case of pET-16b [rcmB]$_{Bmas}$. Subsequently, cultures were incubated for 20 h at 14°C and 120 rpm. All further steps were conducted on ice or at 4°C. Cells were harvested by centrifugation for 15 min at 6,000 $\times$ *g* and washed in 50 mM sodium phosphate, 150 mM NaCl, pH 8.0. Cell disruption was accomplished by use of a mixer mill (model MM 400; Retsch GmbH) with glass beads (212 to 300 μm; Sigma-Aldrich) for 30 min at 30 s^{-1}. The crude extracts containing RcmA or RcmB were loaded onto a 1-ml Ni-nitrilotriacetic acid (NTA) Sepharose gravity flow column (IBA, Goettingen, Germany) equilibrated with Ni-NTA buffer (50 mM sodium phosphate, 300 mM NaCl, 10 mM imidazole, pH 8.0). After the column was washed with Ni-NTA buffer containing 20 mM imidazole over 8 column volumes, elution was performed with 250 mM imidazole over 3 column volumes. The collected protein fractions were analyzed via SDS-PAGE, and the RcmA and RcmB subunits were concentrated using 30- and 10-kDa Viva Spin columns (GE Healthcare), respectively. Finally, protein solutions were diluted 5-fold in conservation buffer (50 mM potassium phosphate, 10% glycerol, pH 7.4).

Cultivation of recombinant *M. extorquens* AM1 strains. For preliminary testing of the product formation of AM1 strains transformed with the pBBR1MCS-3 and pCM80 plasmids carrying different RCM genes, 50 ml of mineral salt medium supplemented with 10 mg liter^{-1} of tetracycline and 3 g liter^{-1} of methanol was inoculated with the respective strains to an optical density of 0.1. During growth of the cultures in shaking flasks at 30°C and 150 rpm for a total time span of 7 days, 3 g liter^{-1} of methanol was added anew and the pH was adjusted to 7.0 by addition of 10% sodium hydroxide after 2, 4, and 6 days.

Precultures for bioreactor experiments were inoculated from a frozen stock containing 1.5 mg of cells in 100 μl of 10% glycerol. After incubation in 50 ml mineral salt medium with tetracycline for 3 days at 30°C and 150 rpm, the cultures served as the inoculum for a bioreactor with an initial working volume of 2 liters (2-liter BioStat B-DCU II; Sartorius Stedim Systems GmbH). The reactor was equipped with a metal stirrer, in- and outlet ports for air, substrate, base (1 M sodium hydroxide), and sampling, as

well as probes for pH and dissolved oxygen. During fermentation, the pH was automatically maintained at 7.0 ± 0.1 by addition of base and the dissolved oxygen level was automatically maintained at 20% ± 5% by adjusting the stirring rate to between 400 and 1,000 rpm and the airflow rate to between 0.2 and 1.0 liter min^{-1}. The substrate solution containing 500 g $liter^{-1}$ of methanol in nitrogen-free mineral salt medium was added by a peristaltic pump with manually preset pumping rates and weighed by precision scales to maintain the methanol concentration within the reactor preferably between 0.5 and 5 g $liter^{-1}$.

For off-line analytics, culture samples were initially centrifuged for 5 min at 13,000 × *g* for separation of the pellet and supernatant. Bacterial dry mass was determined gravimetrically after oven drying for 5 h at 105°C. The concentrations of methanol and 2-HIBA in the supernatant were quantified via HPLC with refractive index detection after separation on a Nucleogel Ion 300 OA column (300 by 7.7 mm; Macherey-Nagel), to which an eluent of 0.01 N sulfuric acid was applied at 0.5 ml per min. The nitrogen concentration was assessed using ammonia test strips (10 to 400 mg $liter^{-1}$ NH_4^+; Merckoquant; Merck). The intracellular PHB content was determined from 5 mg of cells after lyophilization for 24 h. PHB was extracted, and (*R*)-3-hydroxybutyric acid monomers were esterified via hydrochloric acid propanolysis as described before (54). The arising propyl ester was detected by gas chromatography (GC) using a 6890 GC instrument (Agilent) with a Zebron ZB-35 HT Inferno GC column (20 m by 0.18 mm; Phenomenex). For determination of formation and consumption rates and the derived product yields of PHB and 2-HIBA, fermentation data were interpolated by use of a Gompertz function describing an asymmetric saturation curve (OriginPro, version 9.0, software).

Determination of acyl-CoA mutase activity. To investigate the activity of heterologously expressed RCM from *B. massiliosenegalensis* JC6, the purified subunits RcmA and RcmB were incubated in equal molecular amounts of 1 μM in a final volume of 1 ml in reaction buffer (50 mM potassium phosphate, 50 mM Tris, 10% glycerol) with 800 μM coenzyme B_{12} and 1 mM $MgCl_2$ for 5 min at the respective assay temperature as described previously (3). Then, the reaction was started by adding various concentrations of the acyl-CoA ester substrate 2-hydroxyisobutyryl-CoA, (*R*)-3-hydroxybutyryl-CoA, or (*S*)-3-hydroxybutyryl-CoA in reaction buffer (50 mM potassium phosphate, 50 mM Tris, 10% glycerol). pH and temperature optima were assessed by adjusting the pH value from 6.0 to 10.0 and the temperature from 20°C to 50°C. Determination of kinetic parameters was subsequently carried out at pH 7.8 and 35°C. The reactions were stopped by addition of an equal volume of 100 mM acetate, pH 3.5, and incubation for 5 min at 60°C. Substrate and product concentrations were measured via HPLC with photometric detection at 260 nm. Therefore, a Nucleosil 100-5 C_{18} column (250 by 3 mm; Macherey-Nagel) and a mobile phase of 100 mM sodium phosphate, 10 mM tetrabutylammonium hydrogen sulfate, and 20% acetonitrile at pH 4.5 and 0.6 ml per min were applied. Kinetic parameters were calculated by nonlinear regression analysis using the Michaelis-Menten equation (12). For determination of the mutase activity in crude extracts of *M. extorquens* AM1, cells were harvested by centrifugation of fermentation samples for 15 min at 6,000 × *g* and 4°C, washed in 50 mM sodium phosphate, pH 7.0, and disrupted by use of a mixer mill for 30 min at 30 s^{-1}. Cell extracts were used in the enzyme assays to a final protein concentration of 0.4 mg ml^{-1}, and the reactions were performed with 200 μM (*R*)-3-hydroxybutyryl-CoA at pH 7.8 and 30°C.

Reverse transcription-quantitative PCR. For RT-qPCR, fermentation samples of *M. extorquens* AM1 were mixed with 2 volumes of RNAprotect Bacteria reagent (Qiagen), pelleted by centrifugation for 10 min at 5,000 × *g*, and stored at −80°C. Cellular RNA of the frozen pellets was isolated using an RNeasy minikit (Qiagen) according to the protocol of the manufacturer. After DNA digestion with a Turbo DNA-free kit (Thermo Fisher Scientific), 200 ng of RNA of each sample was transcribed into cDNA by application of a RevertAid first-strand cDNA synthesis kit (Thermo Fisher Scientific) and an oligo$(dT)_{18}$ primer. The cDNA directly served as the template for RT-qPCRs in triplicate using iQ SYBR green supermix and a CFX96 real-time system (Bio-Rad). All primers applied for amplification of the reference genes (*recA*, *rpoD*) and target genes (*rcmA*, *rcmB*, *meaH*, *mxaF*, *glyA*, *phaB*, *croR*) are listed in Table 2. The suitability of the reference genes was tested with GenEx software (version 6.1; bioMCC). The qPCR program consisted of an initial denaturation at 95°C for 3 min, followed by incubation for 15 s at 95°C, 60 s at 60°C, and plate read for 40 cycles. Thereafter, a melting curve was recorded from 55 to 95°C with increments of 0.5°C for 5 s. The qPCR results were analyzed with CFX Manager software (Bio-Rad), and the relative ratio of the level of expression of each target gene in comparison to the level of expression of the reference genes was calculated as described by Pfaffl (55).

SUPPLEMENTAL MATERIAL

Supplemental material for this article may be found at https://doi.org/10.1128/AEM.02622-16.

TEXT S1, PDF file, 0.5 MB.

ACKNOWLEDGMENTS

We thank C. Dilßner and M. Neytschev (UFZ) for excellent technical and analytical assistance during the fermentation experiments and synthesis of the acyl-CoA ester substrates. We are also indebted to B. Würz and A. Kölsch (UFZ) for GC analysis and lyophilization of the PHB samples. Finally, we express our sincere thanks to M. E. Lidstrom for kindly providing us with the pCM80 expression vector.

REFERENCES

1. Choi S, Song CW, Shin JH, Lee SY. 2015. Biorefineries for the production of top building block chemicals and their derivatives. Metab Eng 28: 223–239. https://doi.org/10.1016/j.ymben.2014.12.007.
2. Bozell JJ, Petersen GR. 2010. Technology development for the production of biobased products from biorefinery carbohydrates—the US Department of Energy's "top 10" revisited. Green Chem 12:539–554. https://doi.org/10.1039/b922014c.
3. Yaneva N, Schuster J, Schäfer F, Lede V, Przybylski D, Paproth T, Harms H, Müller RH, Rohwerder T. 2012. Bacterial acyl-CoA mutase specifically catalyzes coenzyme B_{12}-dependent isomerisation of 2-hydroxyisobutyryl-CoA and (*S*)-3-hydroxybutyryl-CoA. J Biol Chem 287: 15502–15511. https://doi.org/10.1074/jbc.M111.314690.
4. Kurteva-Yaneva N, Zahn M, Weichler MT, Starke R, Harms H, Müller RH, Sträter N, Rohwerder T. 2015. Structural basis of the stereospecificity of bacterial B_{12}-dependent 2-hydroxyisobutyryl-CoA mutase. J Biol Chem 290:9727–9737. https://doi.org/10.1074/jbc.M115.645689.
5. Rohwerder T, Breuer U, Benndorf D, Lechner U, Müller RH. 2006. The alkyl *tert*-butyl ether intermediate 2-hydroxyisobutyrate is degraded via a novel cobalamin-dependent mutase pathway. Appl Environ Microbiol 72:4128–4135. https://doi.org/10.1128/AEM.00080-06.
6. Madison LL, Huisman GW. 1999. Metabolic engineering of poly(3-hydroxyalkanoates): from DNA to plastic. Microbiol Mol Biol Rev 63: 21–53.
7. Rohwerder T, Müller RH. 2010. Biosynthesis of 2-hydroxyisobutyric acid (2-HIBA) from renewable carbon. Microb Cell Fact 9:13. https://doi.org/10.1186/1475-2859-9-13.
8. Hoefel T, Wittmann E, Reinecke L, Weuster-Botz D. 2010. Reaction engineering studies for the production of 2-hydroxyisobutyric acid with recombinant *Cupriavidus necator* H16. Appl Microbiol Biotechnol 88: 477–484. https://doi.org/10.1007/s00253-010-2739-4.
9. Przybylski D, Rohwerder T, Harms H, Yaneva N, Müller RH. 2013. Synthesis of the building block 2-hydroxyisobutyrate from fructose and butyrate by *Cupriavidus necator* H16. Appl Microbiol Biotechnol 97: 8875–8885. https://doi.org/10.1007/s00253-013-5064-x.
10. Przybylski D, Rohwerder T, Harms H, Müller RH. 2012. Third-generation feed stocks for the clean and sustainable biotechnological production of bulk chemicals: synthesis of 2-hydroxyisobutyric acid. Energy Sustain Soc 2:11. https://doi.org/10.1186/2192-0567-2-11.
11. Przybylski D, Rohwerder T, Dilßner C, Maskow T, Harms H, Müller RH. 2015. Exploiting mixtures of H_2, CO_2, and O_2 for improved production of methacrylate precursor 2-hydroxyisobutyric acid by engineered Cupriavidus necator strains. Appl Microbiol Biotechnol 99:2131–2145. https://doi.org/10.1007/s00253-014-6266-6.
12. Weichler MT, Kurteva-Yaneva N, Przybylski D, Schuster J, Müller RH, Harms H, Rohwerder T. 2015. Thermophilic coenzyme B_{12}-dependent acyl-coenzyme A (CoA) mutase from *Kyrpidia tusciae* DSM 2912 preferentially catalyzes isomerization of (*R*)-3-hydroxybutyryl-CoA and 2-hydroxyisobutyryl-CoA. Appl Environ Microbiol 81:4564–4572. https://doi.org/10.1128/AEM.00716-15.
13. Ramasamy D, Lagier JC, Gorlas A, Raoult D, Fournier PE. 2013. Non contiguous-finished genome sequence and description of *Bacillus massiliosenegalensis* sp. nov. Stand Genomic Sci 8:264–278. https://doi.org/10.4056/sigs.3496989.
14. Dijkhuizen L, Hansen TA, Harder W. 1985. Methanol, a potential feedstock for biotechnological processes. Trends Biol Sci 3:262–267.
15. Olah GA. 2005. Beyond oil and gas: the methanol economy. Angew Chem Int Ed Engl 44:2636–2639. https://doi.org/10.1002/anie.200462121.
16. Schrader J, Schilling M, Holtmann D, Sell D, Villela M, Marx A, Vorholt JA. 2009. Methanol-based industrial biotechnology: current status and future perspectives of methylotrophic bacteria. Trends Biotechnol 27: 107–115. https://doi.org/10.1016/j.tibtech.2008.10.009.
17. Chistoserdova L, Kalyuzhnaya MG, Lidstrom ME. 2009. The expanding world of methylotrophic metabolism. Annu Rev Microbiol 63:477–499. https://doi.org/10.1146/annurev.micro.091208.073600.
18. Peel D, Quayle JR. 1961. Microbial growth on C1 compounds. I. Isolation and characterization of *Pseudomonas* AM 1. Biochem J 81:465–469.
19. Zhu WL, Cui JY, Cui LY, Liang WF, Yang S, Zhang C, Xing XH. 2016. Bioconversion of methanol to value-added mevalonate by engineered *Methylobacterium extorquens* AM1 containing an optimized mevalonate pathway. Appl Microbiol Biotechnol 100:2171–2182. https://doi.org/10.1007/s00253-015-7078-z.
20. Sonntag F, Müller JEN, Kiefer P, Vorholt JA, Schrader J, Buchhaupt M. 2015. High-level production of ethylmalonyl-CoA pathway-derived dicarboxylic acids by *Methylobacterium extorquens* under cobalt-deficient conditions and by polyhydroxybutyrate negative strains. Appl Microbiol Biotechnol 99:3407–3419. https://doi.org/10.1007/s00253-015-6418-3.
21. Peyraud R, Schneider K, Kiefer P, Massou S, Vorholt JA, Portais JC. 2011. Genome-scale reconstruction and system level investigation of the metabolic network of *Methylobacterium extorquens* AM1. BMC Syst Biol 5:189. https://doi.org/10.1186/1752-0509-5-189.
22. Ochsner AM, Sonntag F, Buchhaupt M, Schrader J, Vorholt JA. 2015. *Methylobacterium extorquens*: methylotrophy and biotechnological applications. Appl Microbiol Biotechnol 99:517–534. https://doi.org/10.1007/s00253-014-6240-3.
23. Peyraud R, Kiefer P, Christen P, Massou S, Portais JC, Vorholt JA. 2009. Demonstration of the ethylmalonyl-CoA pathway by using ^{13}C metabolomics. Proc Natl Acad Sci U S A 106:4846–4851. https://doi.org/10.1073/pnas.0810932106.
24. Ivanova EG, Fedorov DN, Doronina NV, Trotsenko YA. 2006. Production of vitamin B_{12} in aerobic methylotrophic bacteria. Mikrobiologiia 75: 570–572.
25. Kovach ME, Elzer PH, Hill DS, Robertson GT, Farris MA, Roop RM, Peterson KM. 1995. Four new derivatives of the broad-host-range cloning vector pBBR1MCS, carrying different antibiotic-resistance cassettes. Gene 166:175–176. https://doi.org/10.1016/0378-1119(95)00584-1.
26. Marx CJ, Lidstrom ME. 2001. Development of improved versatile broad-host-range vectors for use in methylotrophs and other Gram-negative bacteria. Microbiology 147:2065–2075. https://doi.org/10.1099/00221287-147-8-2065.
27. Charbonneau DM, Beauregard M. 2013. Role of key salt bridges in thermostability of *G. thermodenitrificans* EstGtA2: distinctive patterns within the new bacterial lipolytic enzyme subfamily XIII.2. PLoS One 8:e76675. https://doi.org/10.1371/journal.pone.0076675.
28. Kovacic F, Mandrysch A, Poojari C, Strodel B, Jaeger KE. 2016. Structural features determining thermal adaptation of esterases. Protein Eng Des Sel 29:65–76. https://doi.org/10.1093/protein/gzv061.
29. Figueira MM, Laramée L, Murrell JC, Groleau D, Míguez CB. 2000. Production of green fluorescent protein by the methylotrophic bacterium *Methylobacterium extorquens*. FEMS Microbiol Lett 193:195–200. https://doi.org/10.1111/j.1574-6968.2000.tb09423.x.
30. Choi YJ, Bourque D, Morel L, Groleau D, Míguez CB. 2006. Multicopy integration and expression of heterologous genes in *Methylobacterium extorquens* ATCC 55366. Appl Environ Microbiol 72:753–759. https://doi.org/10.1128/AEM.72.1.753-759.2006.
31. Choi YJ, Morel L, Bourque D, Mullick A, Massie B, Míguez CB. 2006. Bestowing inducibility on the cloned methanol dehydrogenase promoter (P_{mxaF}) of *Methylobacterium extorquens* by applying regulatory elements of *Pseudomonas putida* F1. Appl Environ Microbiol 72: 7723–7729. https://doi.org/10.1128/AEM.02002-06.
32. Hu B, Lidstrom ME. 2014. Metabolic engineering of *Methylobacterium extorquens* AM1 for 1-butanol production. Biotechnol Biofuels 7:156. https://doi.org/10.1186/s13068-014-0156-0.
33. Schada von Borzyskowski L, Remus-Emsermann M, Weishaupt R, Vorholt JA, Erb TJ. 2015. A set of versatile brick vectors and promoters for the assembly, expression, and integration of synthetic operons in *Methylobacterium extorquens* AM1 and other alphaproteobacteria. ACS Synth Biol 4:430–443. https://doi.org/10.1021/sb500221v.
34. Chubiz LM, Purswani J, Carroll SM, Marx CJ. 2013. A novel pair of inducible expression vectors for use in *Methylobacterium extorquens*. BMC Res Notes 6:183. https://doi.org/10.1186/1756-0500-6-183.
35. Rohde MT, Paufler S, Harms H, Maskow T. 2016. Calorespirometric feeding control enhances bioproduction from toxic feedstocks—demonstration for biopolymer production out of methanol. Biotechnol Bioeng 113:2113–2121. https://doi.org/10.1002/bit.25986.
36. Merchant SS, Helmann JD. 2012. Elemental economy: microbial strategies for optimizing growth in the face of nutrient limitation. Adv Microb Physiol 60:91–210. https://doi.org/10.1016/B978-0-12-398264-3.00002-4.
37. Bentley WE, Mirjalili N, Andersen DC, Davis RH, Kompala DS. 1990. Plasmid-encoded protein: the principal factor in the "metabolic burden"

associated with recombinant bacteria. Biotechnol Bioeng 35:668–681. https://doi.org/10.1002/bit.260350704.
38. Pasini M, Fernández-Castané A, Jaramillo A, de Mas C, Caminal G, Ferrer P. 2016. Using promoter libraries to reduce metabolic burden due to plasmid-encoded proteins in recombinant *Escherichia coli*. N Biotechnol 33:78–90. https://doi.org/10.1016/j.nbt.2015.08.003.
39. Sonntag F, Buchhaupt M, Schrader J. 2014. Thioesterases for ethylmalonyl-CoA pathway derived dicarboxylic acid production in *Methylobacterium extorquens* AM1. Appl Microbiol Biotechnol 98:4533–4544. https://doi.org/10.1007/s00253-013-5456-y.
40. FitzGerald KA, Lidstrom ME. 2003. Overexpression of a heterologous protein, haloalkane dehalogenase, in a poly-beta-hydroxybutyrate-deficient strain of the facultative methylotroph *Methylobacterium extorquens* AM1. Biotechnol Bioeng 81:263–268. https://doi.org/10.1002/bit.10470.
41. Orita I, Nishikawa K, Nakamura S, Fukui T. 2014. Biosynthesis of polyhydroxyalkanoate copolymers from methanol by *Methylobacterium extorquens* AM1 and the engineered strains under cobalt-deficient conditions. Appl Microbiol Biotechnol 98:3715–3725. https://doi.org/10.1007/s00253-013-5490-9.
42. Chou HH, Chiu HC, Delaney NF, Segrè D, Marx CJ. 2011. Diminishing returns epistasis among beneficial mutations decelerates adaptation. Science 332:1190–1192. https://doi.org/10.1126/science.1203799.
43. Korotkova N, Lidstrom ME. 2001. Connection between poly-β-hydroxybutyrate biosynthesis and growth on C_1 and C_2 compounds in the methylotroph *Methylobacterium extorquens* AM1. J Bacteriol 183:1038–1046. https://doi.org/10.1128/JB.183.3.1038-1046.2001.
44. Laukel M, Rossignol M, Borderies G, Völker U, Vorholt JA. 2004. Comparison of the proteome of *Methylobacterium extorquens* AM1 grown under methylotrophic and nonmethylotrophic conditions. Proteomics 4:1247–1264. https://doi.org/10.1002/pmic.200300713.
45. Okubo Y, Skovran E, Guo X, Sivam D, Lidstrom ME. 2007. Implementation of microarrays for *Methylobacterium extorquens* AM1. OMICS 11:325–340. https://doi.org/10.1089/omi.2007.0027.
46. Suzuki T, Yamane T, Shimizu S. 1986. Mass production of poly-β-hydroxybutyric acid by fully automatic fed-batch culture of methylotroph. Appl Microbiol Biotechnol 23:322–329.
47. Okabe M, Lies D, Kanamasa S, Park EY. 2009. Biotechnological production of itaconic acid and its biosynthesis in *Aspergillus terreus*. Appl Microbiol Biotechnol 84:597–606. https://doi.org/10.1007/s00253-009-2132-3.
48. Lidstrom ME. 2006. Aerobic methylotrophic prokaryotes, p 618–634. *In* Dworkin M, Falkow S, Rosenberg E, Schleifer K-H, Stackebrandt E (ed), The prokaryotes, 3rd ed, vol 2. Ecophysiology and biochemistry. Springer, New York, NY.
49. Zhang S, Kang P, Meyer TJ. 2014. Nanostructured tin catalysts for selective electrochemical reduction of carbon dioxide to formate. J Am Chem Soc 136:1734–1737. https://doi.org/10.1021/ja4113885.
50. Bar-Even A, Noor E, Flamholz A, Milo R. 2013. Design and analysis of metabolic pathways supporting formatotrophic growth for electricity-dependent cultivation of microbes. Biochim Biophys Acta 1827:1039–1047. https://doi.org/10.1016/j.bbabio.2012.10.013.
51. Bar-Even A, Noor E, Lewis NE, Milo R. 2010. Design and analysis of synthetic carbon fixation pathways. Proc Natl Acad Sci U S A 107:8889–8894. https://doi.org/10.1073/pnas.0907176107.
52. Padmakumar R, Gantla S, Banerjee R. 1993. A rapid method for the synthesis of methylmalonyl-coenzyme A and other CoA-esters. Anal Biochem 214:318–320. https://doi.org/10.1006/abio.1993.1494.
53. Choi JH, Kim JH, Daniel M, Lebeault JM. 1989. Optimization of growth medium and poly-β-hydroxybutyric acid production from methanol in *Methylobacterium organophilum*. Kor J Appl Microbiol Bioeng 17:392–396.
54. Riis V, Mai W. 1988. Gas-chromatographic determination of poly-beta-hydroxybutyric acid in microbial biomass after hydrochloric acid propanolysis. J Chromatogr 445:285–289. https://doi.org/10.1016/S0021-9673(01)84535-0.
55. Pfaffl MW. 2001. A new mathematical model for relative quantification in real-time RT-PCR. Nucleic Acids Res 29:e45. https://doi.org/10.1093/nar/29.9.e45.